iScience

CellPress
OPEN ACCESS

Article

Zeb1 regulation of wound-healing-induced inflammation in alkali-damaged corneas

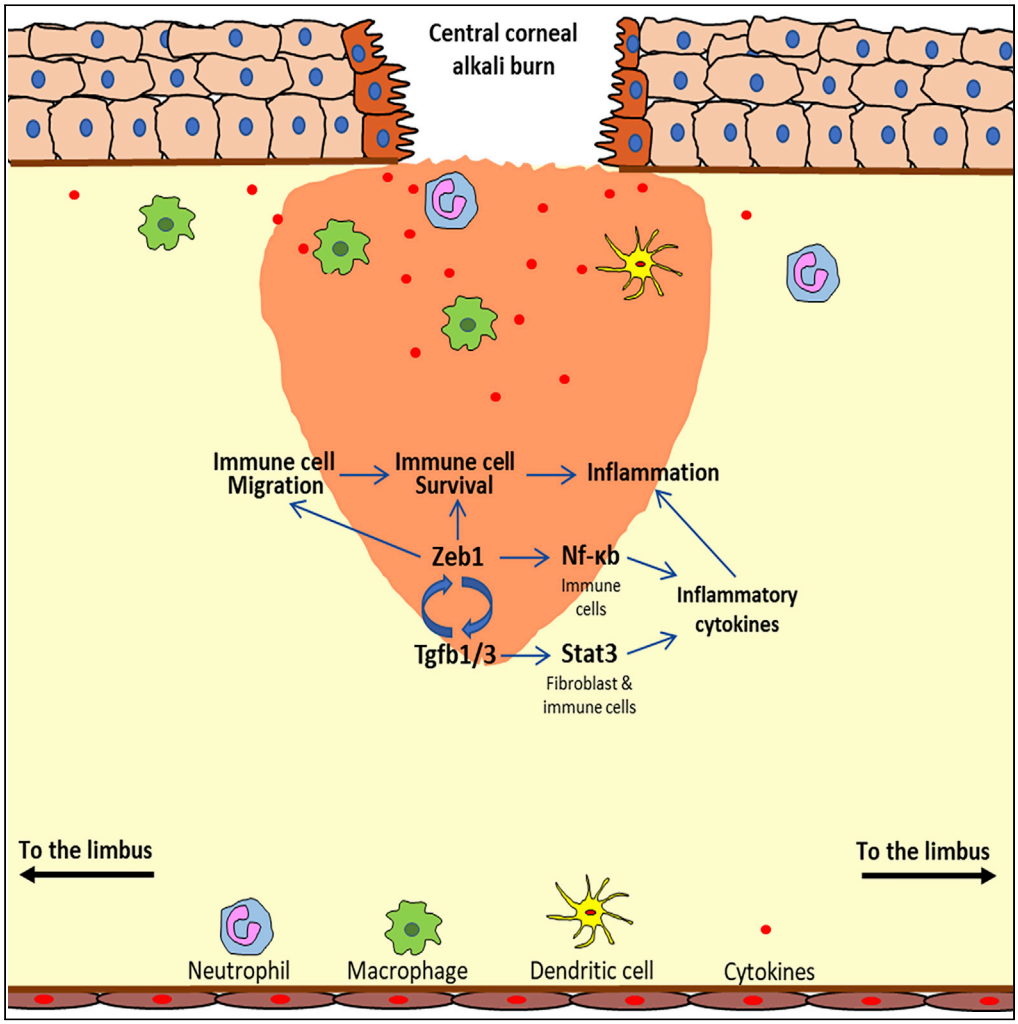

Wei Liang, Yingnan Zhang, Liang Zhou, ..., Douglas C. Dean, Lijun Zhang, Yongqing Liu

dcdean01@louisville.edu (D.C.D.)
lijunzhangw@gmail.com (L.Z.)
y0liu016@louisville.edu (Y.L.)

Highlights

Traumatic wound induces inflammation in the cornea, resulting in vision reduction

Zeb1 is a key factor to retain immune cell viability, mobility, and cytokine expression

Zeb1 regulates cytokine gene expression through both Nf-κb and Stat3 pathways

Inactivation of ZEB1 could be a strategy to treat severe corneal inflammation condition

Liang et al., iScience 25, 104038
April 15, 2022
https://doi.org/10.1016/j.isci.2022.104038

iScience

CellPress
OPEN ACCESS

Article

Zeb1 regulation of wound-healing-induced inflammation in alkali-damaged corneas

Wei Liang,[1,2,6] Yingnan Zhang,[1,3,6] Liang Zhou,[4,5] Xiaoqin Lu,[1,3] Margaret E. Finn,[1,3] Wei Wang,[4] Hui Shao,[4] Douglas C. Dean,[1,3,4,*] Lijun Zhang,[2,*] and Yongqing Liu[1,3,4,7,*]

SUMMARY

The cornea is an avascular tissue for vision clarity. Alkali burn could cause severe traumatic damage on the cornea with inflammation and neovascularization (NV), leading to vision reduction and blindness. Mechanisms underlying corneal inflammation and NV are not as clear. We previously reported that Zeb1 is an important factor in corneal NV, and we sought to clarify whether it is also involved in regulation of corneal inflammation. We analyzed the alkali burn-induced corneal inflammation and wound healing in both $Zeb1^{+/+}$ and $Zeb1^{-/+}$ littermates through a multidisciplinary approach. We provide evidence that Zeb1 forms a positive regulatory loop with Tgfb to regulate early corneal inflammation by maintenance of immune cell viability and mobility and later wound healing by activation of both Nf-κb and Tgfb-related Stat3 signaling pathways. We believe that ZEB1 is a potential therapeutic target, and inactivation of ZEB1 could be a strategy to treat severe corneal inflammation condition.

INTRODUCTION

The cornea is the most upfront ocular tissue. Any trauma on the cornea caused by physical and chemical insults or pathogenic infections could initiate an inflammation and follow-up with a wound healing process that may result in neovascularization (NV) and/or scar formation and thereby lead to vision reduction and even blindness (Wilson, 2020). In fact, corneal trauma-caused complication is the most frequent cause for blindness in the world (Holan et al., 2015). Tissue inflammation starts with the secretion of inflammatory cytokines from stimulated cells and is further enhanced by the recruitment of immune cells either locally and/or mobilized from the bone marrow to produce more local inflammatory cytokines (Wilson, 2020). In vascularized tissues, physical damages often cut off blood supply, leading to a hypoxic microenvironment where the activation of the hypoxia-induced factor HIF1A is responsible for expression of many inflammatory genes (Semenza, 2001). However, this is not the case in the cornea where the oxygen is diffused from the tears through the epithelium and from the anterior chamber fluid through the endothelium (Hassell and Birk, 2010). The basal membrane of the corneal epithelium reserves good amounts of inflammatory cytokines that can be immediately released into the wounding sites when the epithelium breaks to initiate inflammatory signals in the nearby stroma and to recruit immune cells to amplify the signals (Wilson, 2020). The underlying molecular mechanisms for both activation of stromal cells and amplification of the inflammatory signals are not as clear in the cornea, and we sought to clarify if and how the transcription factor ZEB1 regulates corneal inflammation.

ZEB1 is an epithelial-to-mesenchymal transition (EMT) factor involving in cell differentiation and transformation in development and pathogenesis of many diseases including cancer and tissue fibrosis (Sanchez-Tillo et al., 2012). ZEB1 can either repress or promote expression of target genes depending on its interacting partners (Sanchez-Tillo et al., 2012). It often stays on the target genes to silence their transcription when interacting with the C-terminal binding protein (CtBP) and a histone deacetylase (HDAC) whereas also promotes target gene expression when interacting with a DNA demethylase such as P300 (Sanchez-Tillo et al., 2012). Based on the current model, ZEB1 is activated by the transforming growth factor beta (TGFβ) through TGFβ-SMAD signaling pathway (Sanchez-Tillo et al., 2012). Mutations of ZEB1 have been linked to stem cell inefficiency (Wang et al., 2020), immune deficiency (Dean et al., 2015), and corneal endothelial dystrophy (Liu et al., 2008b; Zhang et al., 2021). We and others find that ZEB1 promotes both cell proliferation by inhibiting cyclin-dependent kinase inhibitors (CDKI) (Liu et al., 2008a) and migration by enhancing EMT properties (Chen et al., 2017; Xue et al., 2019), whereas the loss of ZEB1 function mutation

[1]Department of Medicine, University of Louisville School of Medicine, Louisville, KY 40202, USA

[2]Department of Ophthalmology, Third People's Hospital of Dalian, Dalian Medical University, Dalian 116033, China

[3]James Brown Cancer Center, University of Louisville School of Medicine, Louisville, KY 40202, USA

[4]Department of Ophthalmology and Visual Sciences, University of Louisville School of Medicine, Louisville, KY 40202, USA

[5]Department of Ophthalmology, Second Xiangya Hospital of Central South University, Changsha, China

[6]These authors contributed equally

[7]Lead contact

*Correspondence: dcdean01@louisville.edu (D.C.D.), lijunzhangw@gmail.com (L.Z.), y0liu016@louisville.edu (Y.L.)

https://doi.org/10.1016/j.isci.2022.104038

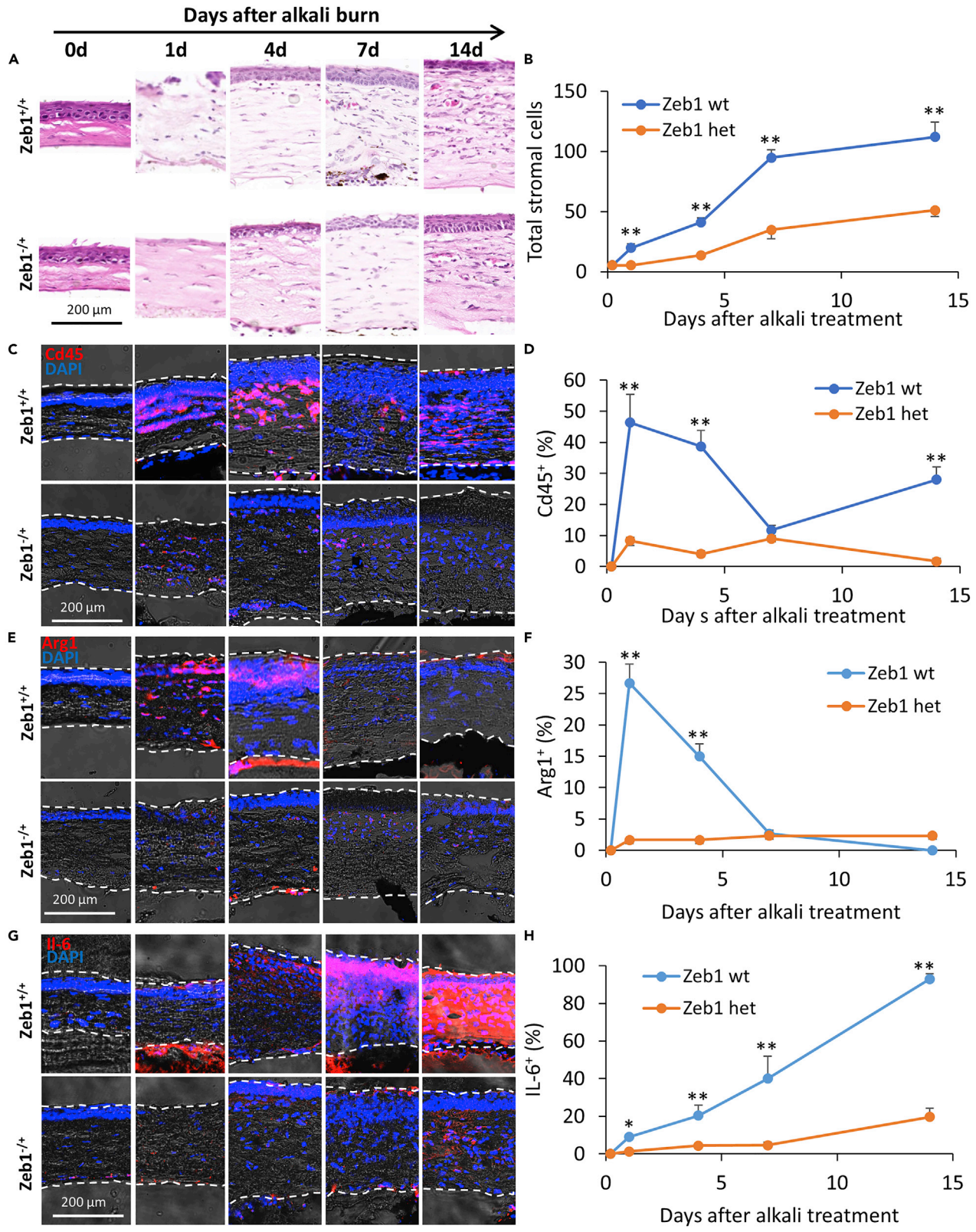
Days after alkali burn
0d
1d
4d
7d
14d
A
Zeb1+/+
Zeb1-/+
200 μm
B
Total stromal cells
Zeb1 wt
Zeb1 het
Days after alkali treatment
C
Cd45
DAPI
D
Cd45+ (%)
Day s after alkali treatment
E
Arg1
DAPI
F
Arg1+ (%)
Days after alkali treatment
G
Il-6
DAPI
H
IL-6+ (%)
Days after alkali treatment

Figure 1. Corneal inflammatory response to the alkali burn

(A) H&E histological staining of paraffin-imbedded corneal tissues at different time points after alkali burn and (B) a graph showing an accumulation of stromal cells in the affected cornea over the same period.

(C–H) Cryosections immunostained with (C and D) the leukocyte marker Cd45, (E and F) the macrophage marker Arg1, (G and H) the inflammatory cytokine IL-6, and their quantitative changes over 14 days after the alkali burn. The y axis of the graphs indicates the percentage (%) of the stained area to the total area of the corneal section detected by ImageJ. The number of the corneas assessed was 3 or 4 (n = 3 or 4). Data are represented as mean ± standard deviation. Zeb1 wild type, Zeb1 wild type or $Zeb1^{+/+}$; Zeb1 het, Zeb1 heterozygous or $Zeb1^{-/+}$; *, $p < 0.05$; **, $p < 0.01$.

leads to cell senescence (Liu et al., 2008a). In adult tissues, abnormal activation of ZEB1 often results in cancer metastasis (Schmalhofer et al., 2009) and scar formation (Petito et al., 2013) that lead to tissue malfunction. ZEB1 is usually expressed in mesenchymal cells including connective tissue cells and immune cells that are not tightly connected with their neighbor cells and mobile. These cells express, synthesize, and secrete a variety of cytokines when stimulated by an environmental stimulus (Liu et al., 2017; Wilson et al., 2001). ZEB1 has been reported to bind and transactivate a group of inflammatory cytokines such as interleukin-1b (IL-1b), IL-6, IL-8, TNFa, CSF2, etc. (Cho et al., 2014; Ramirez-Perez et al., 2020). On the other hand, many cytokines such as TGFβ are also reported to activate expression of ZEB1 through tyrosine kinase receptors, SMAD, NF-κB, and STAT3 signaling pathways (Liu et al., 2017; Sanchez-Tillo et al., 2012; Sato et al., 2005; Tang et al., 2017).

We and others recently reported that ZEB1 promotes tissue NV (Fu et al., 2020b; Jin et al., 2020) and inflammation in colorectal cancer (de Barrios et al., 2019). We discovered that Zeb1 promotes vascular endothelial cell proliferation that contributes to corneal NV (Jin et al., 2020). It is not clear whether inflammatory cytokines that could induce NV affect Zeb1 and/or vice versa in the cornea. Alkali burn could induce both corneal inflammation and NV (Wagoner, 1997). Here, we provide evidence that Zeb1 is indeed involved in wound healing-induced inflammation in the cornea. The underlying mechanisms for Zeb1 regulation of the corneal inflammation are the maintenance of (1) immune cell viability and mobility and (2) the expression of inflammatory cytokines in both immune and fibroblast cells through Nf-κb and Tgfb-activated Stat3 signaling pathways in the alkali burn-induced corneal wound healing.

RESULTS

Alkali burn damages corneal epithelium and induces stromal inflammation

We previously reported that topic application of alkali solution to the mouse cornea would immediately damage the cornea and induce visible neovascularization (NV) in the stroma in 7–14 days (Jin et al., 2020). The alkali burn eradicated the epithelium that completely exposed the stroma on day 1 (Figure 1A). It was followed by epithelial wound healing to restore and to fully reproduce the epithelium in 4 days (Figure 1A). Based on the H&E-stained nuclei, the augmentation of stromal cells was in a slower pace in the first 4 days and then in a more rapid pace thereafter (Figure 1B). The $Cd45^+$ immune cells, recruited from the limbal circulation, infiltrated the stromal tissue starting from the area close to the epithelium to increase the stromal thickness and cell counts (Figures 1C and 1D). The $Arg1^+$ macrophages appeared in 4 days and disappeared thereafter (Figures 1E and 1F). The NV started to be seen near the limbal site in 7 days and would reach the central cornea in about 2 weeks as previously reported (Jin et al., 2020), which coincided with the accumulation of the inflammatory cytokine IL-6 (Figures 1G and 1H). The blood vessels were located close to the epithelium (Figure 1A), indicating that the cytokines that attracted the leukocytes were released initially from the wounded epithelium and the stroma close to the epithelium and then largely from the accumulated immune cells close to the nearby vessels.

Zeb1 haploinsufficiency reduces the inflammatory response of the cornea to the alkali-burn-induced wound healing

We also previously reported that Zeb1 reduction in the Zeb1 heterozygous mice ($Zeb1^{-/+}$) developed corneal NV less severe compared with their wild-type littermates ($Zeb1^{+/+}$) after the alkali burn (Figure 1A) (Jin et al., 2020). To clarify whether such a haploinsufficiency of Zeb1 also reduces the inflammatory response of the cornea to the alkali burn, we compared the alkali-induced inflammatory response in $Zeb1^{-/+}$ mice to that in $Zeb1^{+/+}$ littermates. As Zeb1 null embryos ($Zeb1^{-/-}$) die right before birth, we used $Zeb1^{-/+}$ mice as they develop normally as the $Zeb1^{+/+}$ littermates (Takagi et al., 1998), although their *Zeb1* expression in the cornea is about 50% less than the $Zeb1^{+/+}$ littermates (Jin et al., 2020). The H&E histological and immunostained sections of the corneal tissues demonstrated that Zeb1 haploinsufficiency significantly reduced tissue inflammatory response to the alkali burn, i.e., significant less inflammatory cells

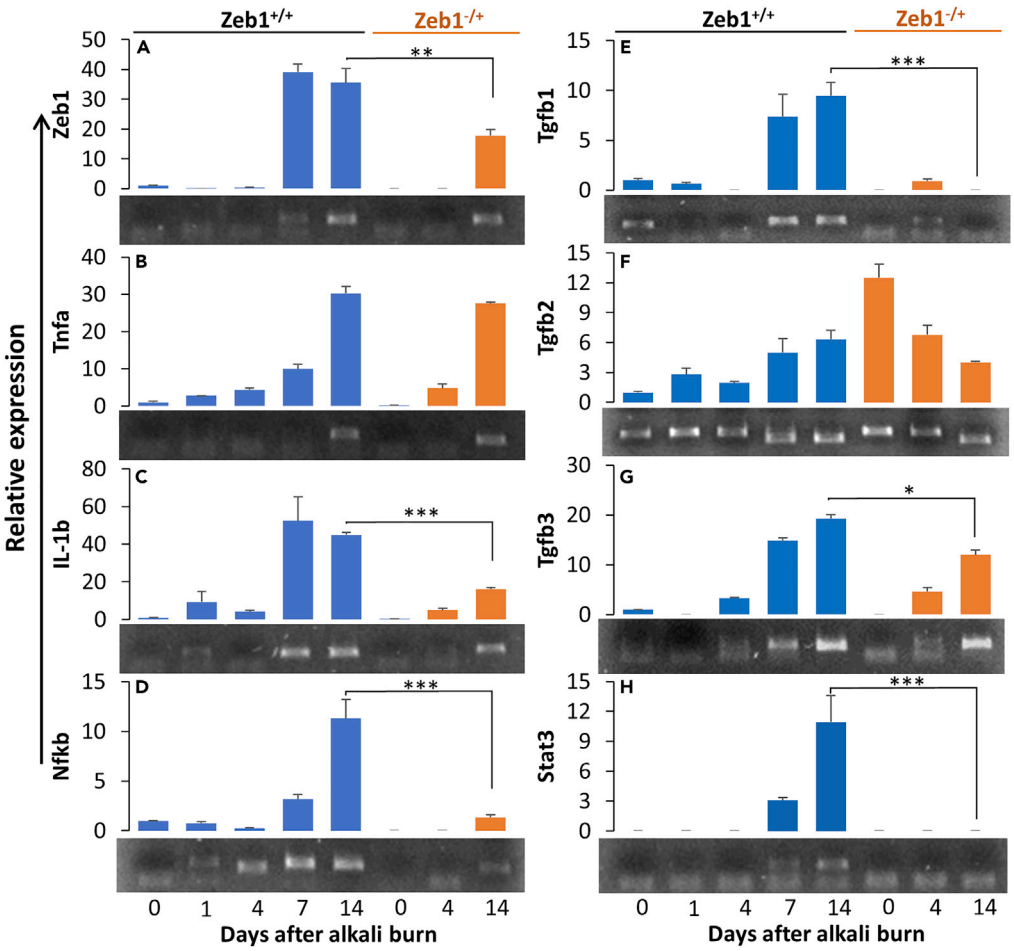

Figure 2. Changes in expression of genes in Zeb1$^{+/+}$ and Zeb1$^{-/+}$ corneas in response to the alkali burn

(A) *Zeb1*; (B) *IL-1b*; (C) *Tnfa*; (D) *NF-κB*; (E) *Tgfb1*; (F) *Tgfb2*; (G) *Tgfb3*; (H) *Stat3*. Six corneas from six mice were collected and mixed for total RNA extraction for qPCR analyses at each time point. An agarose gel image of qPCR amplicons for each gene is attached below the bar graph. Three technical replicates were performed, and the results were presented as mean ± standard deviation. *, $p < 0.05$; **, $p < 0.01$; ***, $p < 0.001$.

(Figures 1A and 1B) including Cd45^{+} leukocytes (Figures 1C and 1D) and Arg1^{+} macrophages (Figures 1E and 1F), and less accumulation of the inflammatory cytokine IL-6 (Figures 1G and 1H) in Zeb1$^{-/+}$ mice compared with Zeb1$^{+/+}$ littermates, suggesting that Zeb1 in the cornea is required for a more severe inflammatory response to the alkali burn.

Alkali burn-induced corneal wound healing activates expression of both Zeb1 and inflammatory cytokines in the cornea

To check whether the alkali burn stimulates Zeb1 expression in the affected corneas and whether Zeb1 expression correlates with the expression of inflammatory cytokines, we prepared total RNA samples from the corneas of both Zeb1$^{+/+}$ and Zeb1$^{-/+}$ at different time points after the alkali burn. We noticed that *Zeb1* message levels were detected low in the untreated wild-type corneal tissues and became indetectable in 1–4 days after the alkali treatment and then increased to higher levels in 7–14 days (Figure 2A). Similar to the expression of *Zeb1* (Figure 2A), the message of the inflammation cytokine *Tnfa* was also low initially until day 7 (Figure 2B). By contrast, *IL-1b* expression was significantly increased on day 1, followed by a reduction, and then increased to the highest level on day 7 after the alkali burn (Figure 2C). The expression of the inflammatory cytokine regulator *Nf-κb* was immediately induced by the alkali burn and gradually increased thereafter to the highest level on day 14 (Figure 2D). Apparently, these cytokines plus IL-6 (Figures 1G and 1H), no matter whether they were induced immediately or not by the alkali burn, were all highly

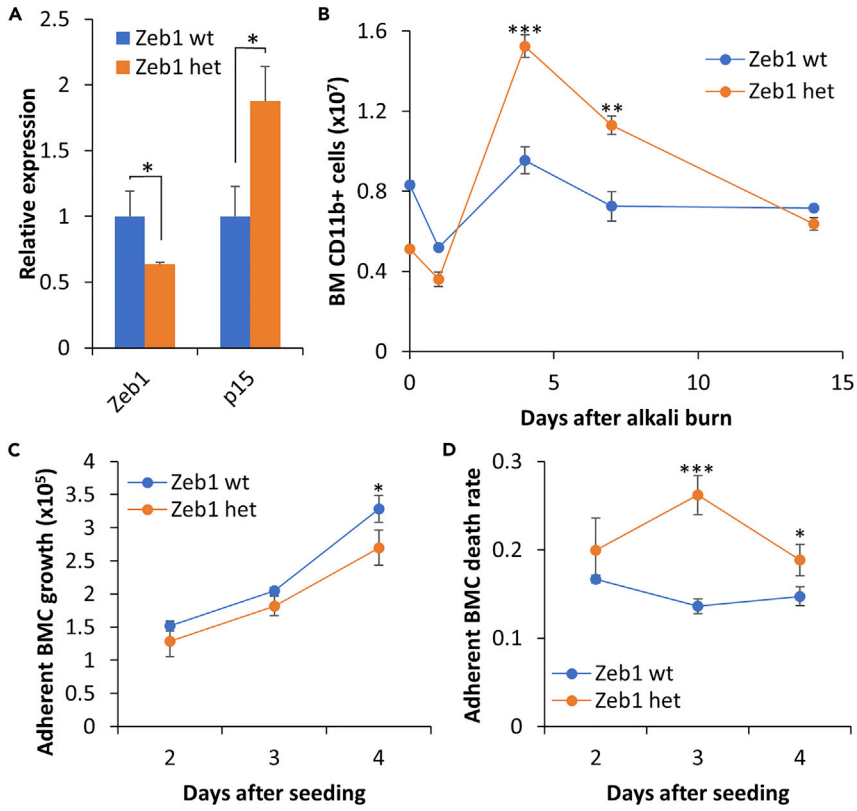

Figure 3. Monoallelic Zeb1 knockout (KO) reduces BMC viability *in vitro*

(A) Expression of *Zeb1* and cyclin-dependent kinase inhibitor *p15* in BMCs of both Zeb1$^{+/+}$ and Zeb1$^{-/+}$ mice detected by qPCR.

(B) Changes in number of Cd11b^{+} BMCs produced in the bone marrow and detected by flow cytometry over the entire course after the alkali burn. The results were calculated from 3–4 mice for each genotype and time point.

(C) 1 × 10^{6} BMCs from both Zeb1$^{+/+}$ and Zeb1$^{-/+}$ mice without alkali burn were cultured in macrophage culture medium for 2–4 days and the adherent BMCs collected by trypsinization and then stained with trypan blue.

The counts of trypan blue negative (i.e. live) BMCs were plotted as cell growth curves, whereas (D) the adherent BMC death rates were calculated on the actual counts of the trypan blue positive (i.e. dead) cells over total counted cells. Data are represented as mean ± standard deviation. BM, bone marrow; BMC, bone-marrow-derived cell; wild type, Zeb1 wild type or Zeb1$^{+/+}$; het, Zeb1 heterozygous or Zeb1$^{-/+}$; *, $p < 0.05$; **, $p < 0.01$; ***, $p < 0.001$.

expressed in later time points, i.e., in 7–14 days after the alkali burn and well coincided with the expression of *Zeb1*, indicating that Zeb1 may either directly or indirectly regulate their expression and/or vice versa. To clarify whether Zeb1 regulates these cytokines upon the alkali burn, our qPCR results demonstrated that in comparison to the Zeb1 wild-type (Zeb1$^{+/+}$) corneas, Zeb1 haploinsufficiency in the Zeb1$^{-/+}$ cornea significantly reduced the expression levels of IL-6 (Figures 1G and 1H), *IL-1b* (Figure 2C) and *Nf-kb* (Figure 2D), suggesting that Zeb1 likely regulates the expression of these inflammatory cytokines in the alkali-burned cornea.

Monoallelic Zeb1 knockout (KO) reduces viability of adherent bone marrow-derived cells (BMCs) in culture

Upon the alkali burn, Zeb1 heterozygous corneas showed significantly less Cd45^{+} leukocytes and Arg1^{+} macrophages than their wild-type littermates (Figures 1E and 1F). It has been reported that complete deletion of Zeb1 (Zeb1$^{-/-}$) significantly reduces T cell production in the embryonic thymus (Dean et al., 2015; Higashi et al., 1997). It seemed therefore that Zeb1$^{-/+}$ mice produced less leukocytes, and/or their mobility was compromised and/or they die much earlier during their migration and at their destination. To validate whether Zeb1$^{-/+}$ mice would produce less Cd11b^{+} myeloid lineages in the bone marrow than Zeb1$^{+/+}$ littermates, we isolated BMCs after the alkali burn at different time points and performed flow cytometric analyses. As expected, the BMCs of monoallelic Zeb1-KO (Zeb1$^{-/+}$) mice expressed less Zeb1 (Figure 3A).

And, Zeb1$^{-/+}$ mice had less Cd11b^{+} BMCs than Zeb1$^{+/+}$ mice initially before and after the alkali burn (Figure 3B). Although the alkali burn decreased the number of Cd11b^{+} BMCs of both Zeb1$^{+/+}$ and Zeb1$^{-/+}$ mice in 1 day likely due to their circulation and deposition to the wounding cornea, the wound healing eventually increased Cd11b^{+} BMCs thereafter until 14 days after the alkali burn (Figure 3B), which is likely due to a compensational cell production in the bone marrow. Surprisingly, the BMC production rate was higher in monoallelic Zeb1-KO mice compared with their wild-type littermates (Figure 3B), suggesting that less Cd45^{+} and Arg1^{+} cells in the Zeb1$^{-/+}$ cornea after the alkali burn (Figures 1C–1F) is not due to their decrease in BMC production. Then, how does the reduction of Zeb1 cause less presence of Cd45^{+} leukocytes in the alkali burn-damaged cornea (Figures 1C and 1D)? We suspect that those Zeb1$^{-/+}$ BMCs would have problems in surviving the circulation and/or deposition.

Although immature monocytes can be proliferative even *in vitro* (Lari et al., 2009), neutrophils and macrophages are the most eminent inflammatory immune cells circulated to the affected sites right after tissue damage, and they are not proliferative in periphery tissues and would die in about 5 days after fully matured (Basu et al., 2002). To validate whether Zeb1$^{-/+}$ BMCs decrease their viability, we cultured them under the macrophage culture condition, i.e., in 30% L929-conditioned medium, and found that the augmentation of live BMCs in Zeb1$^{-/+}$ mice was decreased compared with that in Zeb1$^{+/+}$ mice (Figure 3C). This result was further confirmed by *in vitro* BMC death rates estimated by trypan blue staining (Figure 3D), suggesting that less Cd45^{+} leukocytes, mostly Arg1^{+} macrophages, may senesce immediately after matured in the circulation and die *in situ* after deposited to periphery tissues as the cornea. As reported previously (Liu et al., 2008a), the reduction of Zeb1 increased the expression of cyclin-dependent kinase inhibitors such as p15 (Figure 3A), which is likely the cause for BMC death.

Reduction of Zeb1 expression reduces BMC mobility

As mentioned earlier, the Zeb1 might also promote tissue inflammation by increasing mobility of leukocytes to the affected sites. To clarify whether BMC mobility is affected *in vitro*, we performed a cell migration assay on the monolayer culture of BMCs and found that the mobility of Zeb1$^{-/+}$ BMCs was significantly reduced compared with the Zeb1$^{+/+}$ cells (Figures 4A–4C), suggesting that Zeb1 regulates tissue inflammation also at least partly through increasing immune cell mobility to the affected sites. The mechanism underlying Zeb1 promotion of cell mobility appeared to be by Zeb1 upregulation of the expression of the cytoskeletal components vimentin (*Vim*), actin alpha (*Acta1*), and integrin alpha (*Itga3*) (Figure 4D). Taken together, we conclude that Zeb1 promotion of corneal inflammation was likely through maintaining immune cell viability and mobility in the cornea after the alkali burn.

Zeb1 regulates expression of inflammatory cytokines

As demonstrated earlier, the reduction of Zeb1 in the monoallelic Zeb1$^{-/+}$ corneas delayed the onset and reduced the expression of some inflammatory cytokines at both mRNA and protein levels compared with the biallelic Zeb1$^{+/+}$ corneas (Figures 1G, 1H, 2B, and 2C). It appeared that Zeb1 might regulate expression of inflammatory cytokines—another potential mechanism underlying Zeb1 regulation of immune cell migration to the affected sites. It is known that alkali burn-caused corneal wounding releases inflammatory cytokines such as IL-1 initially from the epithelium to induce apoptosis of the underneath stromal keratocytes, to signal recruitment of immune cells from the circulation to the wounded sites (Ljubimov and Saghizadeh, 2015). The keratocyte is thereby a critical component in the cornea for initiation of corneal inflammation upon wounding. As the keratocyte is basically a corneal stromal fibroblast (Ljubimov and Saghizadeh, 2015) and it is difficult to isolate and to culture mouse primary keratocytes, we used mouse embryonic fibroblast (MEF) as a mimicry for the keratocyte to study its biological function in response to the inflammatory ligand lipopolysaccharide (LPS), an endotoxin and major component of the outer membrane of the Gram-negative bacteria. We compared the expression of the inflammatory cytokine genes in Zeb1$^{+/+}$ MEFs versus in the complete Zeb1-KO (Zeb1$^{-/-}$) MEFs and PBS control versus LPS-treated cells. No *Zeb1* was expressed in Zeb1$^{-/-}$ MEFs as previously reported (Liu et al., 2008a) regardless of the LPS treatment, whereas LPS significantly stimulated *Zeb1* expression in Zeb1$^{+/+}$ MEFs (Figure 5). Except for *IL-1b* that was not expressed in MEFs although the LPS treatment significantly induced its expression in both Zeb1$^{+/+}$ and Zeb1$^{-/-}$ MEFs, Zeb1-KO reduced the expression of *Tnfa* and *Tgfb1/2* cytokines in both control and LPS-treated MEFs (Figure 5). Regardless of Zeb1 expression, LPS treatment significantly increased the expression of the tested cytokines except for *Tgfb3* in Zeb1$^{+/+}$ MEFs (Figure 5). These results suggest that LPS-induced inflammatory cytokine expression could comprise two parts: one is independent of Zeb1 regulation, whereas the other is Zeb1 dependent. Thereby the LPS-stimulated Tlr4-conjugated

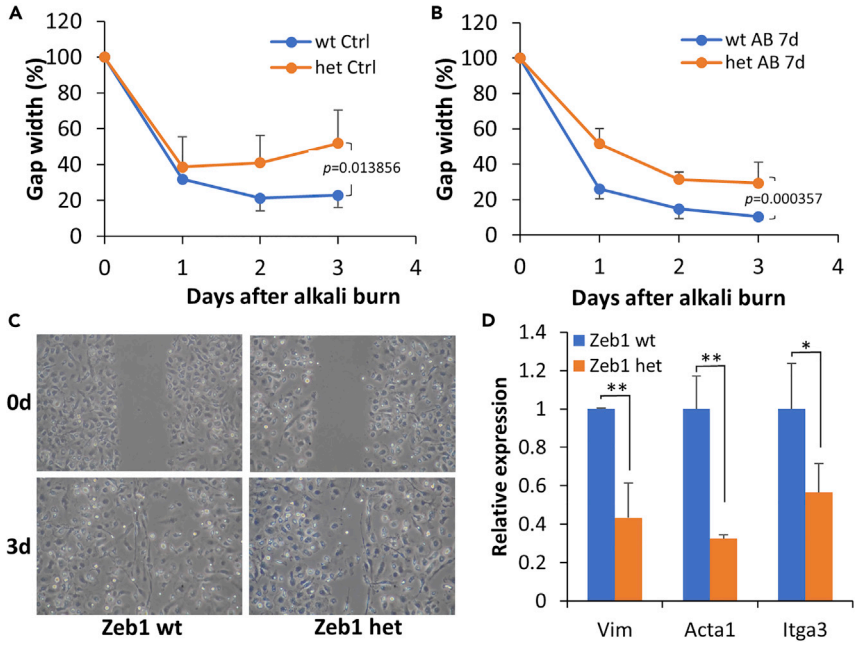

Figure 4. Zeb1 promotes BMC mobility *in vitro*

Monolayer-cultured BMCs were first treated with mitomycin for 1 h to completely stop cell proliferation and then 3 straight scratch lines were created with a 200-μL pipet tip on each culture plate.

(A and B) The gap width of cultured Zeb1$^{+/+}$ and Zeb1$^{-/+}$ BMCs isolated from animals with and without alkali burn was photographed and measured every day for 3 days using ImageJ.

(C) Representative images of the monolayer-cultured Zeb1$^{+/+}$ and Zeb1$^{-/+}$ BMCs in 0 and 3 days after the straight line was made.

(D) Expression of the cytoskeletal genes vimentin (*Vim*), actin alpha 1 (*Acta1*), and integrin alpha 3 (*Itga3*) in BMCs isolated from control animals without alkali burn. Data are represented as mean ± standard deviation. Ctrl, PBS control; AB, alkali burn; Zeb1 wild type, Zeb1$^{+/+}$; Zeb1 het, Zeb1$^{-/+}$; *, $p < 0.05$; **, $p < 0.01$.

activation of signaling pathways such as Nf-κb activation (Kawai and Akira, 2007) may or may not be involved in Zeb1-regulated cytokine expression in the alkali-induced corneal inflammation.

Alkali burn and LPS induction of Zeb1 may be through Tgfb signaling pathway

As demonstrated earlier, Zeb1 expression could be induced by wound healing in the alkali-burned corneas detected by qPCR (Figure 2A) and by LPS treatment in the cultured MEFs detected by both qPCR (Figure 5) and WB (Figure 6A) that positively correlated with the increase in inflammatory cytokines (Figures 2 and 5). To clarify the causal relationship between Zeb1 and cytokines, we detailed the sequential events over the alkali burn-caused corneal wound healing. Alkali burn immediately damaged the corneal tissue and caused a minor augmentation wave of the cytokines *IL-1b*, *Tnfa*, *Tgfb2*, and their regulator *Nf-κb* on day 1 when *Zeb1* expression was actually decreased (Figure 2), suggesting that Zeb1 may not be required for induction of inflammatory cytokines at least in the early phase of corneal wound healing process. These early cytokines are supposed to be released from local cells in the cornea, i.e., the epithelial, stromal fibroblasts, and immune cells (Ljubimov and Saghizadeh, 2015). Zeb1 expression was however significantly increased a week later after the alkali burn when the tested cytokines were all highly expressed (Figure 2). The mechanism underlying the wound healing upregulation of Zeb1 in the cornea is not known. However, it is known that the cytokine TGFβ can induce ZEB1 expression through TGFβ receptor to activate SMAD transcription factors that bind to and thereby activate *ZEB1* gene expression (Sanchez-Tillo et al., 2011, 2012). To check whether TGFβ induces *Zeb1* expression in immune cells and/or fibroblasts, we treated the monolayer-cultured BMCs and MEFs with 25 ng/mL TGFβ1 for 16 h. As a result, TGFβ1 boosted *Zeb1* expression in the MEFs but not in the BMCs (Figure 6C). As the LPS induction of cytokines was regardless of Zeb1 expression in MEFs (Figure 5), it seemed that the LPS induction of Zeb1 in MEFs (Figure 5) and the wound healing induction of *Zeb1* in the cornea (Figure 2A) was at least partly through the Tgfb signaling pathway.

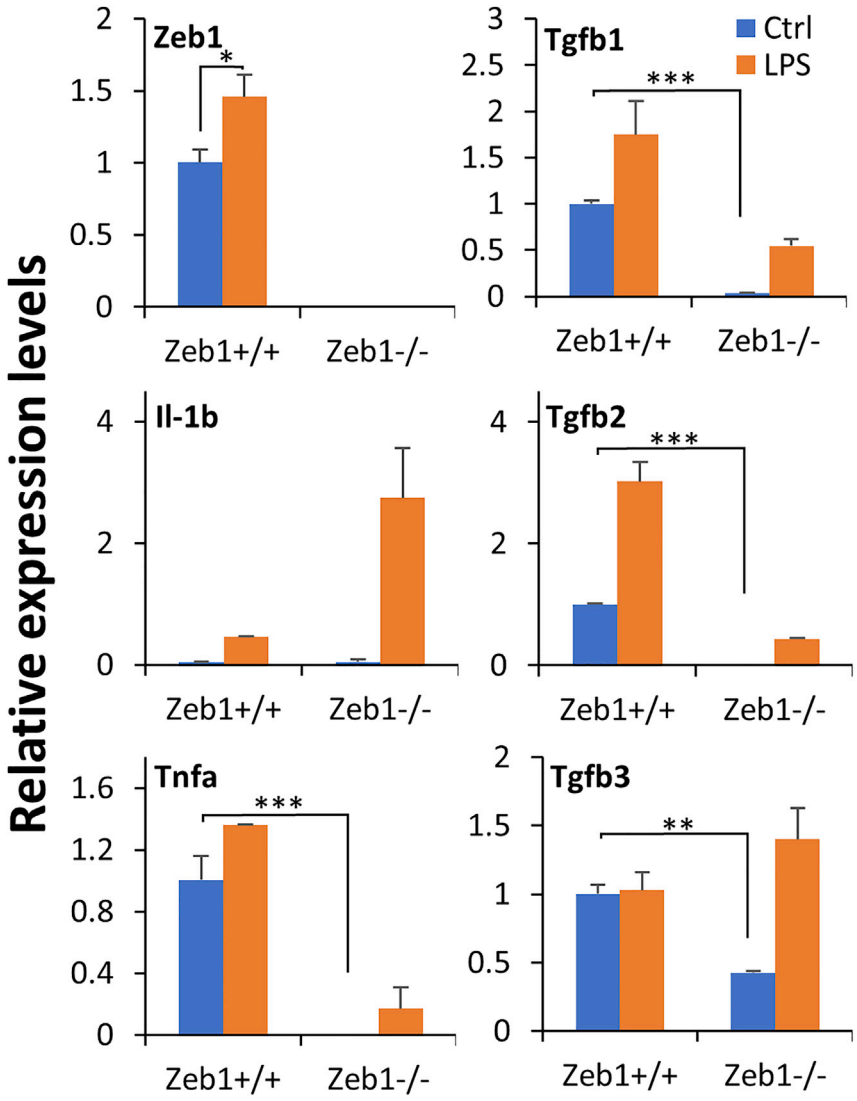

Figure 5. Zeb1-KO in MEFs affects expression of inflammation-associated genes in response to the LPS treatment *in vitro*

The expression of the indicated genes was detected by qPCR, and their expression levels were normalized to the house-keeping gene *Gapdh*. Data are represented as mean ± standard deviation. *, $p < 0.05$; **, $p < 0.01$; ***, $p < 0.001$; Ctrl, PBS control; LPS, lipopolysaccharide.

Zeb1 may directly and indirectly upregulate expression of cytokines through Nf-κb and Stat3 activation

It is of notice that the reduction of Zeb1 did reduce expression of *Tnfa*, *Tgfb1/2/3* in $Zeb1^{-/-}$ MEFs (Figure 5) and *IL-1b*, *Tgfb1/3* in $Zeb1^{-/+}$ corneas (Figure 2), suggesting that Zeb1 might directly and/or indirectly regulate these cytokines. Also, the amounts of Zeb1 protein detected by WB increased significantly in $Zeb1^{+/+}$ BMCs and MEFs upon LPS treatment although no Zeb1 protein was detected in both $Zeb1^{-/+}$ BMCs and $Zeb1^{-/-}$ MEFs no matter whether they were treated with LPS or not (Figure 6A), suggesting that LPS induction of inflammatory cytokines may or may not be through upregulation of Zeb1. To validate whether Zeb1 binds to the putative promoters of the above cytokine genes and their regulator genes, i.e., *Nf-κb* and *Stat3*, we conducted a chromatin immunoprecipitation (ChIP) assay using MEF chromatin and anti-Zeb1 rabbit polyclonal serum as previously reported (Liu et al., 2008a, 2009, 2013). As results, we found that Zeb1 bound to the promoters of *Tgfb1/3* and *Nf-κb* genes (Figure 6B) and thereby evidenced it may directly regulate their expression.

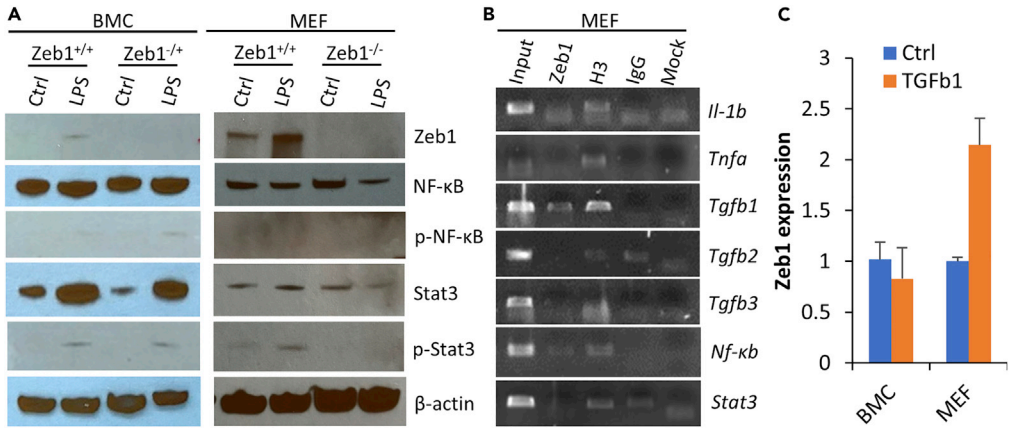

Figure 6. Molecular mechanisms underlying Zeb1 regulation of alkali-induced corneal inflammation

(A) BMCs and MEFs of both Zeb1 wild type ($Zeb1^{+/+}$) and Zeb1-KO ($Zeb1^{-/+}$ or $Zeb1^{-/-}$) were monolayer cultured and treated with or without 1 μg/mL LPS for 1 h. Total proteins were extracted from these cells for WB analyses for the indicated proteins.

(B) Chromatin immunoprecipitation (ChIP) assessments to identify Zeb1 binding to the putative promoter sequences of the indicated genes. Input, 1/10 of the initial chromatin used for immunoprecipitation; Zeb1, the anti-Zeb1 rabbit-serum-precipitated chromatin; H3, anti-pan histone 3 as a positive control; IgG, rabbit pre-serum as a negative control; Mock, without any antibodies.

(C) *Zeb1* expression detected by qPCR in both BMCs and MEFs upon 25 ng/mL of TGFβ1 treatment for 16 h. Ctrl, PBS control. p-Nf-κb, phosphorylated NF-κB; p-Stat3, phosphorylated Stat3. Data are represented as mean ± standard deviation.

It is also known that TGFβ activates TGFβ-activated kinase 1 (TAK1) that would further activate the downstream kinase IKK to phosphorylate the NF-κB inhibitor IκBα, leading to ubiquitin-dependent IκBα degradation and NF-κB activation (Sato et al., 2005). As a major regulator for inflammatory cytokine gene expression, Nf-κb increased significantly, and its activation form p-Nf-κb (p65) was also induced in BMCs upon LPS treatment (Figure 6A) as expected. In contrast, Nf-κb expression at both message in the cornea (Figure 2D) and protein levels and the activation of p-Nf-κb were decreased when Zeb1 was reduced in BMCs (Figure 6A). Obviously, Zeb1 binds to *Nf-κb* gene to directly increase its expression and to indirectly activate its phosphorylation likely through TGFβ pathway (Sato et al., 2005) (Figure 7A). As opposite to BMCs, LPS treatment decreased the amount of Nf-κb protein and did not activate it by phosphorylation in MEFs (Figure 6A), suggesting that Nf-κb activation is unlikely a mechanism to increase inflammatory cytokine expression in the fibroblasts.

In search for a mechanism for Zeb1 to regulate inflammatory cytokine expression in keratocytes/fibroblasts, we turned our attention to JAK-STAT3 signaling pathway, as JAK-STAT3 activation is an essential response to stresses (Bharadwaj et al., 2020) including wound healing (Song et al., 2017). As a result, we found that Stat3 was significantly induced at the same time when Zeb1 was significantly upregulated in the alkali-burned corneas (Figure 2H). Also significantly, Stat3 was activated by LPS-induced phosphorylation of Tyr705 in the LPS-treated BMCs and MEFs. More importantly, reduction of Zeb1 in the monoallelic Zeb1-KO corneas and fibroblasts diminished Stat3 activation (Figures 2H and 6A), suggesting that the Jak/Stat3 signaling is another Zeb1-regulated pathway to upregulate inflammatory cytokines in the alkali burned cornea. However, Zeb1 was not found to bind and thereby to directly regulate *Stat3* (Figure 6B). Nevertheless, both IL-6 and *Tgfb* were induced in 7 days following the alkali burn, and the reduction of Zeb1 reduced their expression at the same time in monoallelic Zeb1-KO corneas (Figures 1G, 2E, and 2G). This result suggests Zeb1 may indirectly regulate expression of *Stat3* through upregulation of IL-6 (Figures 1G and 1H) and Tgfb (Figures 2E and 2G) to activate Stat3 signaling pathway in the later phase of the alkali-burn-induced corneal wound healing (Figure 7A), as both IL-6 and Tgfb were reported previously to be the major cytokines for activation of JAK-STAT3 (Bharadwaj et al., 2020; Tang et al., 2017).

DISCUSSION

Zeb1 regulates early alkali burn-induced corneal inflammation by maintaining immune cell viability and mobility

We previously discovered that Zeb1 was involved in alkali burn-induced corneal neovascularization (NV), a serious condition that may lead to blindness if not properly treated, by activating vascular endothelial cell

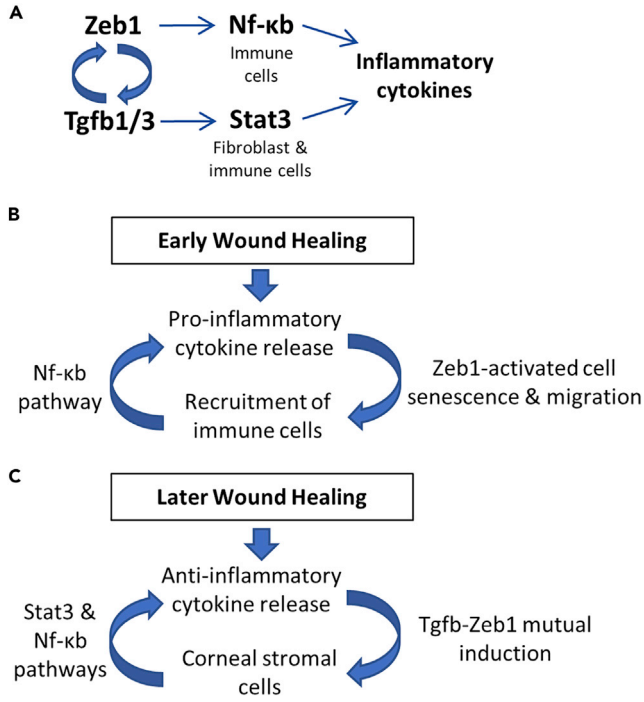

Figure 7. Schematic diagrams to elucidate the mechanisms underlying Zeb1 regulation of inflammation

(A) Molecular mechanisms depicting Zeb1 regulation of inflammatory cytokines through NF-κB and Stat3 regulatory pathways.

(B) Zeb1-activated BMC viability, mobility, and (C) expression of inflammatory cytokines in the early phase and later phase of the alkali-burn-induced corneal wound healing, respectively.

proliferation; and the inhibition of Zeb1 activation by the ZEB1-CtBP inhibitor NSC 95397 could significantly reduce the corneal NV (Jin et al., 2020). It is known that NV goes with tissue inflammation and is often caused by a traumatic wounding, and mouse corneal alkali burn is a well-documented animal model to study corneal wound healing and NV (Anderson et al., 2014). In this study, we found that the alkali burn-induced corneal inflammation was clearly divided into two phases—the early phase until day 4 when immune cells were accumulated locally and the later phase on day 7 and thereafter when NV was established and inflammatory cytokines were accumulated in the affected sites (Figure 1). Intriguingly, monoallelic Zeb1-KO significantly reduced the alkali burn-induced corneal inflammation over the entire course (Figure 1). To clarify the mechanisms underlying Zeb1 regulation of corneal inflammation, we detailed the expression of Zeb1 and inflammatory cytokines in the cornea (Figure 2) and found that in the early phase of the corneal inflammation, Zeb1 expression did not positively correlate with the accumulation of inflammatory cytokines such as *IL-1b* and *Tnfa* (Figures 2A–2C) and $Cd45^+$ immune cells (Figures 1C and 1D). This result suggested that Zeb1 unlikely regulates the early corneal inflammation through regulating the expression of the inflammatory cytokines. Indeed, our ChIP assays demonstrated that Zeb1 did not bind to and thereby unlikely activate both *IL-1b* and *Tnfa* genes (Figure 6B). Then, how did Zeb1 promote the alkali burn-induced corneal inflammation? We thereafter found that Zeb1 could significantly enhance BMC viability and mobility, thereby believing that Zeb1 promotion of the early wound healing-induced corneal inflammation was through maintaining immune cell survival after BMC departing from the bone marrow, getting into the circulation, and finally depositing to the cornea (Figure 7B)

Zeb1 regulates later alkali burn-induced inflammation by activation of Tgfb-related signaling pathways

As we reported here, the Zeb1 was significantly upregulated by the alkali burn-induced inflammation on day 7 and thereafter (Figure 2A) and by the LPS treatment in the fibroblasts and BMCs (Figure 6A) including macrophage cells as reported by others (Li et al., 2015; Rossol et al., 2011). TGFβ is a major cytokine known to bind to its type 2 receptor to initiate signaling cascades to phosphorylate (1) SMAD to induce ZEB1 expression (Sanchez-Tillo et al., 2012), (2) TAK1 and IKK to activate NF-κB (Sato et al., 2005), and (3) JAK

to activate STAT3 (Tang et al., 2017) for upregulation of multiple inflammatory cytokines including IL-1b and TNFa (Sato et al., 2005; Tang et al., 2017). In addition, ZEB1 has also been evidenced to upregulate TGFβ expression (Fu et al., 2020a). It appears that TGFβ signaling and ZEB1 activation form a positive regulatory loop (Fu et al., 2020a). We confirmed that the addition of TGFβ1 to the culture media activated Zeb1 expression in the fibroblasts (Figure 6C) and heterozygous Zeb1 significantly reduced *Tgfb1* and *Tgfb3* expression in the later phase of the alkali burn-induced corneal wound healing (Figures 2E–2G). TGFβ isoforms (β1, β2, and β3) are critical cytokines involved in tissue wound healing process; they facilitate early recruitment of immune cells and later prompt expression of key components of extracellular matrix (ECM), improve angiogenesis, and stimulate contraction of fibroblasts to enable wound closure (Pakyari et al., 2013). We demonstrated in this study that *Tgfb2* was highly expressed in the cornea (Figure 2F), whereas the alkali burn immediately diminished and then increased the expression of *Tgfb1/3* (Figures 2E–2G). Interestingly, the "normal" variant of *Tgfb2* detected by the larger size of the amplicon in the early corneal wound healing shifted to the smaller size variant (Figures 2E and 2F). We do not know how these two *Tgfb2* variants are generated and what biological function(s) they may play. It seemed that the larger size *Tgfb2* variant presented in the cornea before and right after alkali-burn-induced wound healing, suggesting it may play a pro-inflammation defense role in the cornea, whereas the smaller size *Tgfb2* variant and *Tgfb1/3* were mainly induced in the later phase of alkali-burn-induced corneal wound healing, suggesting they may play a critical role in anti-inflammation tissue repair (Figure 7C).

Zeb1 indirectly regulates inflammatory cytokines likely through the upregulation and/or activation of the inflammation regulators Nf-κb and Stat3

LPS can induce inflammatory responses both *in vivo* and *in vitro* by upregulation of multiple inflammatory cytokines in immune cells such as neutrophils and macrophages through the Toll-like receptor 4 (TLR4) signaling pathway to activate three major transcription factors (TFs)—NF-κB, AP1, and IRF3—to bind and upregulate downstream inflammatory cytokine genes (Liu et al., 2017). Alkali burn-induced corneal inflammation may also go through the same Tlr4 signaling pathway to activate inflammatory cytokines and perhaps Zeb1 as well. In other words, Zeb1 could be upregulated by one or more of these LPS-activated TFs, located downstream of the Tlr4 signaling pathway. We therefore sought to find whether the putative promoter region of *Zeb1* gene contains any specific consensus DNA binding sequences of these TFs. Unfortunately, no such consensus sequence for the three TFs was identified in the *Zeb1* promoter region (data not shown) and thereby unlikely for these LPS-activated TFs binding to the *Zeb1* promoter to induce *Zeb1* expression. In contrast, we did provide some evidence that Zeb1 could bind to and transactivate *Nf-κb* (Figure 6B) and monoallelic Zeb1-KO significantly reduced the expression of *NF-κB* in the cornea (Figure 2D), suggesting that Zeb1 might positively regulate *Nf-κb* and thereby contribute to the upregulation of the inflammatory cytokine expression. As expected, we confirmed that Zeb1 significantly upregulated and activated Nf-κb in BMCs, but not in MEFs *in vitro* (Figure 6A), thereby believing that Zeb1 regulation of the inflammatory cytokine expression in the later phases of the alkali-burn-induced corneal inflammation was through Zeb1 activation of Nf-κb pathway in immune cells (Figure 7A). Stat3 also appeared to be a critical regulator in the later phases of the alkali-burn-induced corneal inflammation (Figure 2H), and Zeb1 was required for Stat3 activation, i.e., the phosphorylation of Tyr705 in the fibroblasts (Figure 6A) despite Zeb1 was not detected to bind to and transactivate *Stat3* gene (Figure 6B). We concluded that Zeb1 regulation of the inflammatory cytokine expression in the later phases of the alkali-burn-induced corneal inflammation was at least partly through Tgfb activation of Stat3 pathway (Figures 7A–7C).

Limitations of the study

In this study, we utilized a regular Zeb1-KO mouse strain whose pups could not survive birth if both Zeb1 copies are completely erased. Although Zeb1 heterozygous pups survive birth and develop "normally," they did show an irregular inflammatory response to the corneal alkali burn. We have elucidated the reduction in Zeb1 expression affects viability and mobility of the adherent BMCs by which Zeb1 could affect the inflammation in the cornea. What we do not know, however, is whether the reduction of Zeb1 in heterozygous ($Zeb1^{-/+}$) mice might affect other tissues and/or cells and thereby contribute to the irregular inflammatory response in the cornea. Thus, to clarify this issue, a conditional Zeb1-KO mouse strain where Zeb1 could be deleted in a cell-specific fashion is required for further investigation.

STAR★METHODS

Detailed methods are provided in the online version of this paper and include the following:

SUPPLEMENTAL INFORMATION

Supplemental information can be found online at https://doi.org/10.1016/j.isci.2022.104038.

ACKNOWLEDGMENTS

This work was supported by the National Natural Science Foundation of China (82171032 L.Z.), the Natural Science Foundation of Liaoling Province (201800209, 201602210, and 20180550976 to L.Z.), National Institutes of Health (R01EY026158 and R01EY030933 to D.C.D., P20GM103453 to Y.L.), Basic Research Grant of University of Louisville School of Medicine (E0819 to Y.L.), and James Graham Brown Cancer Center of University of Louisville Directed Gift Pilot Project Program (G1627 to Y.L.).

AUTHOR CONTRIBUTIONS

W.L. and Y.Z.: performed most of the experiments, collected and analyzed the data, wrote the manuscript; L.Z., X.L. and M.E.F.: assisted in cell culture, RNA extraction, and western blot analysis; W.W. and H.S.: analyzed the data; D.C.D, L.Z. and Y.L.: designed experiments, analyzed the data, and wrote the manuscript. All authors read and approved the final manuscript.

DECLARATION OF INTERESTS

The authors declare no competing financial interests.

Received: September 24, 2021
Revised: December 24, 2021
Accepted: March 3, 2022
Published: April 15, 2022

REFERENCES

Anderson, C., Zhou, Q., and Wang, S. (2014). An alkali-burn injury model of corneal neovascularization in the mouse. J. Vis. Exp. 51159. https://doi.org/10.3791/51159.

Basu, S., Hodgson, G., Katz, M., and Dunn, A.R. (2002). Evaluation of role of G-CSF in the production, survival, and release of neutrophils from bone marrow into circulation. Blood *100*, 854–861. https://doi.org/10.1182/blood.v100.3.854.

Bharadwaj, U., Kasembeli, M.M., Robinson, P., and Tweardy, D.J. (2020). Targeting janus kinases and signal transducer and activator of transcription 3 to treat inflammation, fibrosis, and cancer: rationale, progress, and caution. Pharmacol. Rev. *72*, 486–526. https://doi.org/10.1124/pr.119.018440.

Chen, Y., Lu, X., Montoya-Durango, D.E., Liu, Y.H., Dean, K.C., Darling, D.S., Kaplan, H.J., Dean, D.C., Gao, L., and Liu, Y. (2017). ZEB1 regulates multiple oncogenic components involved in uveal melanoma progression. Sci. Rep. *7*, 45. https://doi.org/10.1038/s41598-017-00079-x.

Cho, J.S., Kang, J.H., Um, J.Y., Han, I.H., Park, I.H., and Lee, H.M. (2014). Lipopolysaccharide induces pro-inflammatory cytokines and MMP production via TLR4 in nasal polyp-derived fibroblast and organ culture. PLoS One *9*, e90683. https://doi.org/10.1371/journal.pone.0090683.

de Barrios, O., Sanchez-Moral, L., Cortes, M., Ninfali, C., Profitos-Peleja, N., Martinez-Campanario, M.C., Siles, L., Del Campo, R., Fernandez-Acenero, M.J., Darling, D.S., et al. (2019). ZEB1 promotes inflammation and progression towards inflammation-driven carcinoma through repression of the DNA repair glycosylase MPG in epithelial cells. Gut *68*, 2129–2141. https://doi.org/10.1136/gutjnl-2018-317294.

Dean, K.C., Huang, L., Chen, Y., Lu, X., and Liu, Y. (2015). An Rb1-dependent amplification loop between Ets1 and Zeb1 is evident in thymocyte differentiation and invasive lung adenocarcinoma. BMC Mol. Biol. *16*, 8. https://doi.org/10.1186/s12867-015-0038-4.

Fu, R., Li, Y., Jiang, N., Ren, B.X., Zang, C.Z., Liu, L.J., Lv, W.C., Li, H.M., Weiss, S., Li, Z.Y., et al. (2020a). Inactivation of endothelial ZEB1 impedes tumor progression and sensitizes tumors to conventional therapies. J. Clin. Invest. *130*, 1252–1270. https://doi.org/10.1172/JCI131507.

Fu, R., Lv, W.C., Xu, Y., Gong, M.Y., Chen, X.J., Jiang, N., Xu, Y., Yao, Q.Q., Di, L., Lu, T., et al. (2020b). Endothelial ZEB1 promotes angiogenesis-dependent bone formation and reverses osteoporosis. Nat. Commun. *11*, 460. https://doi.org/10.1038/s41467-019-14076-3.

Hassell, J.R., and Birk, D.E. (2010). The molecular basis of corneal transparency. Exp. Eye Res. *91*, 326–335. https://doi.org/10.1016/j.exer.2010.06.021.

Higashi, Y., Moribe, H., Takagi, T., Sekido, R., Kawakami, K., Kikutani, H., and Kondoh, H. (1997). Impairment of T cell development in deltaEF1 mutant mice. J. Exp. Med. *185*, 1467–1479.

Holan, V., Trosan, P., Cejka, C., Javorkova, E., Zajicova, A., Hermankova, B., Chudickova, M., and Cejkova, J. (2015). A comparative study of the therapeutic potential of mesenchymal stem cells and limbal epithelial stem cells for ocular surface reconstruction. Stem Cells Transl. Med. *4*, 1052–1063. https://doi.org/10.5966/sctm.2015-0039.

Jin, L., Zhang, Y., Liang, W., Lu, X., Piri, N., Wang, W., Kaplan, H.J., Dean, D.C., Zhang, L., and Liu, Y. (2020). Zeb1 promotes corneal neovascularization by regulation of vascular endothelial cell proliferation. Commun. Biol. *3*, 349. https://doi.org/10.1038/s42003-020-1069-z.

Kawai, T., and Akira, S. (2007). Signaling to NF-kappaB by toll-like receptors. Trends Mol. Med. *13*, 460–469. https://doi.org/10.1016/j.molmed.2007.09.002.

Lari, R., Kitchener, P.D., and Hamilton, J.A. (2009). The proliferative human monocyte subpopulation contains osteoclast precursors. Arthritis Res. Ther. *11*, R23. https://doi.org/10.1186/ar2616.

Li, J., Qian, W., Xu, Y., Chen, G., Wang, G., Nie, S., Shen, B., Zhao, Z., Liu, C., and Chen, K. (2015). Activation of RAW 264.7 cells by a polysaccharide isolated from Antarctic bacterium Pseudoaltermonas sp. S-5. Carbohydr. Polym. *130*, 97–103. https://doi.org/10.1016/j.carbpol.2015.04.070.

Liu, Y., El-Naggar, S., Darling, D.S., Higashi, Y., and Dean, D.C. (2008a). Zeb1 links epithelial-mesenchymal transition and cellular senescence. Development *135*, 579–588. https://doi.org/10.1242/dev.007047.

Liu, Y., Peng, X., Tan, J., Darling, D.S., Kaplan, H.J., and Dean, D.C. (2008b). Zeb1 mutant mice as a model of posterior corneal dystrophy. Invest. Ophthalmol. Vis. Sci. *49*, 1843–1849. https://doi.org/10.1167/iovs.07-0789.

Liu, Y., Ye, F., Li, Q., Tamiya, S., Darling, D.S., Kaplan, H.J., and Dean, D.C. (2009). Zeb1 represses Mitf and regulates pigment synthesis, cell proliferation, and epithelial morphology. Invest. Ophthalmol. Vis. Sci. *50*, 5080–5088. https://doi.org/10.1167/iovs.08-2911.

Liu, Y., Mukhopadhyay, P., Pisano, M.M., Lu, X., Huang, L., Lu, Q., and Dean, D.C. (2013). Repression of Zeb1 and hypoxia cause sequential mesenchymal-to-epithelial transition and induction of aid, Oct4, and Dnmt1, leading to immortalization and multipotential reprogramming of fibroblasts in spheres. Stem Cells *31*, 1350–1362. https://doi.org/10.1002/stem.1382.

Liu, T., Zhang, L., Joo, D., and Sun, S.C. (2017). NF-kappaB signaling in inflammation. Signal Transduct. Target. Ther. *2*, 17023. https://doi.org/10.1038/sigtrans.2017.23.

Ljubimov, A.V., and Saghizadeh, M. (2015). Progress in corneal wound healing. Prog. Retin. Eye Res. *49*, 17–45. https://doi.org/10.1016/j.preteyeres.2015.07.002.

Pakyari, M., Farrokhi, A., Maharlooei, M.K., and Ghahary, A. (2013). Critical role of transforming growth factor beta in different phases of wound healing. Adv. Wound Care (New Rochelle) *2*, 215–224. https://doi.org/10.1089/wound.2012.0406.

Petito, R.B., Amadeu, T.P., Pascarelli, B.M., Jardim, M.R., Vital, R.T., Antunes, S.L., and Sarno, E.N. (2013). Transforming growth factor-beta1 may be a key mediator of the fibrogenic properties of neural cells in leprosy. J. Neuropathol. Exp. Neurol. *72*, 351–366. https://doi.org/10.1097/NEN.0b013e31828bfc60.

Ramirez-Perez, S., Hernandez-Palma, L.A., Oregon-Romero, E., Anaya-Macias, B.U., Garcia-Arellano, S., Gonzalez-Estevez, G., and Munoz-Valle, J.F. (2020). Downregulation of inflammatory cytokine release from IL-1beta and LPS-stimulated PBMC orchestrated by ST2825, a MyD88 dimerisation inhibitor. Molecules *25*, 4322. https://doi.org/10.3390/molecules25184322.

Rossol, M., Heine, H., Meusch, U., Quandt, D., Klein, C., Sweet, M.J., and Hauschildt, S. (2011). LPS-induced cytokine production in human monocytes and macrophages. Crit. Rev. Immunol. *31*, 379–446. https://doi.org/10.1615/critrevimmunol.v31.i5.20.

Sanchez-Tillo, E., Siles, L., de Barrios, O., Cuatrecasas, M., Vaquero, E.C., Castells, A., and Postigo, A. (2011). Expanding roles of ZEB factors in tumorigenesis and tumor progression. Am. J. Cancer Res. *1*, 897–912.

Sanchez-Tillo, E., Liu, Y., de Barrios, O., Siles, L., Fanlo, L., Cuatrecasas, M., Darling, D.S., Dean, D.C., Castells, A., and Postigo, A. (2012). EMT-activating transcription factors in cancer: beyond EMT and tumor invasiveness. Cell. Mol. Life Sci. *69*, 3429–3456. https://doi.org/10.1007/s00018-012-1122-2.

Sato, S., Sanjo, H., Takeda, K., Ninomiya-Tsuji, J., Yamamoto, M., Kawai, T., Matsumoto, K., Takeuchi, O., and Akira, S. (2005). Essential function for the kinase TAK1 in innate and adaptive immune responses. Nat. Immunol. *6*, 1087–1095. https://doi.org/10.1038/ni1255.

Schmalhofer, O., Brabletz, S., and Brabletz, T. (2009). E-cadherin, beta-catenin, and ZEB1 in malignant progression of cancer. Cancer Metastasis Rev. *28*, 151–166. https://doi.org/10.1007/s10555-008-9179-y.

Schneider, C.A., Rasband, W.S., and Eliceiri, K.W. (2012). NIH Image to ImageJ: 25 years of image analysis. Nat. Methods. *9*, 671–675.

Semenza, G.L. (2001). Regulation of hypoxia-induced angiogenesis: a chaperone escorts VEGF to the dance. J. Clin. Invest. *108*, 39–40. https://doi.org/10.1172/JCI13374.

Song, Q., Xie, Y., Gou, Q., Guo, X., Yao, Q., and Gou, X. (2017). JAK/STAT3 and Smad3 activities are required for the wound healing properties of Periplaneta americana extracts. Int. J. Mol. Med. *40*, 465–473. https://doi.org/10.3892/ijmm.2017.3040.

Takagi, T., Moribe, H., Kondoh, H., and Higashi, Y. (1998). DeltaEF1, a zinc finger and homeodomain transcription factor, is required for skeleton patterning in multiple lineages. Development *125*, 21–31.

Tang, L.Y., Heller, M., Meng, Z., Yu, L.R., Tang, Y., Zhou, M., and Zhang, Y.E. (2017). Transforming growth factor-beta (TGF-beta) directly activates the JAK1-STAT3 Axis to induce hepatic fibrosis in coordination with the SMAD pathway. J. Biol. Chem. *292*, 4302–4312. https://doi.org/10.1074/jbc.M116.773085.

Wagoner, M.D. (1997). Chemical injuries of the eye: current concepts in pathophysiology and therapy. Surv. Ophthalmol. *41*, 275–313. https://doi.org/10.1016/s0039-6257(96)00007-0.

Wang, X., Xu, H., Cheng, C., Ji, Z., Zhao, H., Sheng, Y., Li, X., Wang, J., Shu, Y., He, Y., et al. (2020). Identification of a Zeb1 expressing basal stem cell subpopulation in the prostate. Nat. Commun. *11*, 706. https://doi.org/10.1038/s41467-020-14296-y.

Wilson, S.E. (2020). Corneal wound healing. Exp. Eye Res. *197*, 108089. https://doi.org/10.1016/j.exer.2020.108089.

Wilson, S.E., Mohan, R.R., Mohan, R.R., Ambrosio, R., Jr., Hong, J., and Lee, J. (2001). The corneal wound healing response: cytokine-mediated interaction of the epithelium, stroma, and inflammatory cells. Prog. Retin. Eye Res. *20*, 625–637. https://doi.org/10.1016/s1350-9462(01)00008-8.

Xue, Y., Zhang, L., Zhu, Y., Ke, X., Wang, Q., and Min, H. (2019). Regulation of proliferation and epithelial-to-mesenchymal transition (EMT) of gastric cancer by ZEB1 via modulating Wnt5a and related mechanisms. Med. Sci. Monit. *25*, 1663–1670. https://doi.org/10.12659/MSM.912338.

Zhang, Y., Liu, X., Liang, W., Dean, D.C., Zhang, L., and Liu, Y. (2021). Expression and function of ZEB1 in the cornea. Cells *10*. https://doi.org/10.3390/cells10040925.

STAR★METHODS

KEY RESOURCES TABLE

REAGENT or RESOURCE	SOURCE	IDENTIFIER
Antibodies		
Rabbit polyclonal Zeb1 anti-serum	Dr. Douglas Darling	N/A
Rabbit polyclonal Arg1 antibody	Novus Biologicals	Cat.# NBP1 - 32731
Goat polyclonal IL-6 antibody	Santa Cruz Biotechnology	Cat.# sc-1265
Rat monoclonal CD45 antibody	eBioscience	Cat.# 14-0451-81
Rabbit polyclonal NF-κB (p65) antibody	Cell Signaling	Cat.# 8242T
Rabbit polyclonal p-NF-κB (p65) antibody	Abclonal	Cat.# AP0123
Mouse monoclonal Stat3 antibody	Cell Signaling	Cat.# 9139S
Mouse monoclonal p-Stat3 (Tyr705) antibody	Cell Signaling	Cat.# 4113S
Mouse monoclonal β-Actin antibody	Sigma	Cat.# A1978
Mouse monoclonal CD11b antibody	eBioscience	Cat.# RM2820
Rabbit monoclonal H3 antibody	Abcam	Cat.# ab176842
Chemicals, peptides, and recombinant proteins		
Lipopolysaccharide (LPS)	Sigma-Aldrich	Cat.# L6529
Transforming growth factor beta (TGFb)	R&D Systems	Cat.# 240-B
Mitomycin C	Sigma-Aldrich	Cat.# M5353
Trypan blue solution	Sigma-Aldrich	Cat.# 93595
Critical commercial assays		
Red blood cell (RBC) lysis buffer	eBioscience	Cat.# 00-4333-57
Enhanced chemiluminescence (ECL) detection reagents	Cytiva	Cat.# RPN2134
Nuclear dye Hoechst 33342	ThermoFisher	Cat.# 62249
Experimental models: Cell lines		
Mouse embryonic fibroblasts (MEF) of both Zeb1 wildtype ($Zeb1^{+/+}$) and knockout (KO, $Zeb1^{-/-}$)	This paper	N/A
Mouse bone marrow-derived cells (BMC) of both Zeb1 wildtype ($Zeb1^{+/+}$) and heterozygous ($Zeb1^{-/+}$)	This paper	N/A
Experimental models: Organisms/strains		
$Zeb1^{tm1Yhi}$/$Zeb1^{tm1Yhi}$ Mus musculus Genetic Background: B6.129P2-Zeb1	Mouse Genome Informatics (MGI)	RRID:MGI:3653696
Oligonucleotides		
Primers, see Tables S1 and S2	This paper	N/A
Software and algorithms		
ImageJ	Schneider et al., 2012	https://imagej.nih.gov/ij/
FlowJo	Tree Star Inc.	http://www.treestar.com/

RESOURCE AVAILABILITY

Lead contact

Further information and requests for data should be directed to and will be fulfilled by the lead contact Yongqing Liu (y0liu016@louisville.edu).

Materials availability

This study did not generate new unique reagents.

Data and code availability

Data reported in this paper will be shared by the lead contact upon request. This paper does not report original code. Any additional information required to reanalyze the data reported in this paper is available from the lead contact upon request.

EXPERIMENTAL MODEL AND SUBJECT DETAILS

The initial Zeb1 knockout (KO) mouse strain was created with a genetic background of both B6 and S129 and characterized by Dr. Y Higashi (Higashi et al., 1997). We maintain this strain in the lab after imported from the creator by breeding Zeb1$^{-/+}$ littermates with B6 mice for many years. As complete Zeb1-KO animal (Zeb1$^{-/-}$) cannot survive birth, the born pups are either Zeb1 wildtype (Zeb1$^{+/+}$) or heterozygous mutant (Zeb1$^{-/+}$). The heterozygous mice grow seemingly normal under regular housing condition. Tail tips of 1–2 weeks old pups are collected for genomic DNA isolation. The genotyping is performed with a pair of primers originally designed by the creator: Hig F 5′- AGCACTATTCTCCGCTACTCCAC and TM1 5′- ACCGCACCTGGTTTACGACACTC to identify the mutants using a regular PCR program with exception of 70°C for both anneal and extension steps for 1 min altogether. The right PCR amplicon size is 193 bp. Adult (6–8 weeks old) Zeb1 heterozygous mice (Zeb1$^{-/+}$) and their wildtype littermates (Zeb1$^{+/+}$) of both sexes were used for the study. This animal study was conducted according to the policies and guidelines set forth by the Institutional Animal Care and Use Committee (IACUC #: 20722) and approved by the University of Louisville, Kentucky, USA.

METHOD DETAILS

Murine model of alkali-induced corneal wound healing

Adult (6–8 weeks old) Zeb1 heterozygous mice (Zeb1$^{-/+}$) and their wildtype littermates (Zeb1$^{+/+}$) of both sexes were anesthetized by an intraperitoneal (IP) injection of 100 mg/kg ketamine and 5 mg/kg xylazine and the alkali-induced corneal wound healing model was created as previously reported (Jin et al., 2020). Briefly, a 2-mm diameter filter disc with 2.5 μL of 1N NaOH was placed on the central cornea of one eye followed by a thorough rinse with PBS whereas the other eye was treated with PBS in the same way as a control. Four or six mice per time point and per genotype were used for corneal section or total RNA extraction, respectively.

Cell culture and treatments

Mouse embryonic fibroblasts (MEFs) were prepared from E17.5 Zeb1$^{+/+}$ and Zeb1$^{-/-}$ embryos (Liu et al., 2008a). For mouse bone marrow-derived cell (BMC) preparation, 3–4 adult Zeb1$^{+/+}$ and Zeb1$^{-/+}$ mice for each time point after the alkali burn were euthanized by CO_2 in a sealed container and their femur and tibia bones of rear legs were isolated and cut at both ends under sterile conditions. The BMCs were flushed out using a 10-mL syringe with a 23-gauge needle and then passed through a 70 μm cell strainer into a 50-mL tube. The BMCs were spun down at 1,500 rpm for 5 min and red blood cells were removed by resuspension in the RBC lysis buffer (eBioscience Cat. # 00-4333-57) for 5 min. After neutronization with equal amount of fetal bovine serum (FBS), the BMCs were spun down and resuspended in PBS and then counted with a hemocytometer and stained for flow cytometric analysis and for culture. For BMC culture, 1x10^6 cells were seeded per well in a 6-well plate. The adherent BMCs were collected by trypsinization in 2 days after seeding, and live and dead cells were counted following staining with 0.4% trypan blue for 3 min at RT. The actual counts of the trypan blue negative live BMCs in 3 replicate wells were plotted as a cell growth curve over next 3 days while BMC death rates were calculated on the actual counts of the trypan blue positive cells over total counted cells. The MEFs were cultured in DMEM medium with 10% FBS whereas BMCs were cultured in 30% L929 cell culture-conditioned DMEM with 10% FBS. The above media were mixed with 1% antibiotics and refreshed every 3 days. Both confluent MEFs and BMCs were treated with either 1 μg/mL of lipopolysaccharide (LPS, Sigma Cat. # L6529) for 1 hour or 25 ng/mL of TGFβ1 (R&D Systems Cat. # 240-B) for 16 hours for cell inflammatory response or Zeb1 activation, respectively.

Flow cytometry

Aliquots of the above 1x10^6 isolated BMCs were first blocked with CD32 and then stained with Alexa Fluor 488-conjugated CD11b (eBioscience Cat. # RM2820) for 30 mins at room temperature. Data collection and analysis were performed on a FACScaliber flow cytometer using FlowJo software (Ashland, OR).

Cell migration assay

Monolayer-cultured BMCs at confluence were treated with 5 μg/ml mitomycin C for 2 hours at 37°C to completely stop cell proliferation and then washed with PBS, followed by making 3 straight scratch lines using a 200P pipette tip, and photographed under an inverted microscope every day at the same location. Width of the scratched gaps for each treatment was measured using ImageJ and the invert of the width measurement was served as a gap closing rate.

Total RNA extraction and real-time quantitative PCR (qPCR)

Total RNA was extracted from homogenized corneal tissues and cultured cells with TRIzol solution. After cDNA was synthesized with the Invitrogen RT kit (Invitrogen), SYBR Green real-time PCR was performed with Stratagene Mx3000P Real-Time PCR system (Jin et al., 2020; Liu et al., 2008a). The sequences and the amplicon sizes of qPCR primers are listed in Table S1. Three independent cell samples or a mixed tissue sample of 6 corneas, each in technical triplicate, were analyzed for each qPCR condition. PCR programs were setup as previous described (Liu et al., 2008a). All PCR products were confirmed by size on 1.5% agarose gels.

Chromatin immunoprecipitation (ChIP) assays

ChIP assays were as previously described (Liu et al., 2008a). Briefly, 1% formaldehyde was used to crosslink genomic DNA of wildtype MEF cells. The chromatin was sheared by sonication to an average length of 500–1000 bp. Primers and antibodies are shown in Table S2 and key resources table, respectively. Input was 1/10 of the initial amount of chromatin used to bind to the anti-Zeb1 serum. Equal amount of the pre-serum (IgG) was used as a negative control whereas the pan histone 3 antibody (abcam Cat. # ab176842) was used as a positive control.

Total protein extraction and western blot (WB)

Cultured MEFs and BMCs treated with 1 μg/mL of LPS or PBS were lysed in protein extraction lysis buffer (RIPA buffer: 150 mM, 5 mM EDTA, 50 mM Tris-HCl pH 8.0, 1% NP-40) on ice for 20 min, followed by a 10-min centrifugation at 13,000 rpm. The amounts of total protein were quantified. A 4–21% gradient SDS-PAGE gel was loaded with 15 μg of the above protein samples, and electrophoresis was performed at 120 V for 60 min. The proteins in the gel were transferred to a PVDC membrane at 4°C overnight. The membrane was incubated in a 5% milk blocking solution and then with number of primary antibodies (key resources table) in the blocking solution at 4°C overnight. The amounts of the tested proteins on the membrane were visualized with the Amersham ECL kit (Cat. # RPN 2106) and detected by an X-ray film.

Tissue sectioning and immunostaining

Enucleated eyeballs were sagittal cut into 2 halves – one for paraffin-embedded section whereas the other for cryosection. The whole eyeball sections were immunostained as described previously (Jin et al., 2020). All primary antibodies are described in key resources table. Cryosections on glass slides were incubated with antibodies at 4°C overnight, and after 3 washes with PBS, followed by an incubation with 1:500 diluted secondary antibodies conjugated with either Alexa Fluor®-568 or Alexa Fluor®-488 (Invitrogen) together with the nuclear dye Hoechst 33342 at room temperature for 60 min. After 3 washes with PBS, the slides were mounted with coverslips using an anti-fade medium (Fisher), and images were captured with a Nikon confocal microscope. We classified the whole corneal section into 3 segments: center, transit and limbal areas and selected the transit segment for assessment, data collection and statistical analysis.

QUANTIFICATION AND STATISTICAL ANALYSIS

Student's *t* test or one-way ANOVA analysis were conducted for two or three independent animal or cell samples, respectively after an F-test confirmation that the comparable samples have an equal level of variance. All values in the graphs are presented as means ± standard deviations. '***' means p-value < 0.001, '**' means p-value < 0.01, whereas '*' means p-value < 0.05. For *in vitro* studies, results were obtained from at least 3 independent experiments of three technical replicates.